Nemets Effect in Deuteron Breakup by Heavy Nuclei*

C. L. FINK, B. L. COHEN, J. C. VAN DER WEERD, AND R. J. PETTY
Department of Physics, University of Pittsburgh, Pittsburgh, Pennsylvania 15213

(Received 5 May 1969)

Nemets *et al.* have suggested that deuteron breakup by heavy nuclei may be appreciably different in closed-shell nuclei from that in neighboring non-closed-shell nuclei because of differences in the diffuseness of the nuclear surface; we refer to this as the Nemets effect. Their experimental evidence, based on measurements at 13.6 MeV in the Ca-Ni region, has been reinvestigated with a more favorable experimental arrangement. It was found that (d, pn) and (d, np) reactions are responsible for a large fraction of the events; they seem to account for most of the differences observed, so there is no good evidence for the effect in this region. However, a study with 17- and 14.5-MeV deuterons on Pb^{208}, Bi^{209}, Au^{197}, and Pt^{198} revealed a strong Nemets effect, with Pb^{208} having a cross section 1.2 to 2.5 times larger than the others. Since a Nemets effect could not be explained if the breakup were by Coulomb forces, nuclear forces must contribute strongly. From this, it is deduced that the usual method for determining the radius at which breakup occurs is invalid. An alternative treatment based on the difference between the neutron and proton nuclear potentials is given, and it is concluded that the breakup occurs at $r \simeq 1.3A^{1/3}$ F.

INTRODUCTION

THE breakup of a deuteron into a neutron and a proton in the field of a heavy nucleus (without excitation of that nucleus) has been studied widely, both experimentally[1–3] and theoretically.[4] The process has a large cross section, and the neutron and proton angular distributions are strongly peaked in the forward direction. There has been a large amount of qualitative discussion of the question of whether the breakup is due principally to nuclear or electromagnetic forces, although it is clear that the two processes are coherent and both undoubtedly contribute. One widely used analysis technique is to estimate the radius R_B at which the breakup occurs from the energy distribution of the emitted particles. Since this method will be discussed and questioned in this paper, we give a derivation here.

As a deuteron of incident energy E_d approaches a nucleus, it is decelerated by the electric field so that its energy at R_B is $E_d - Ze^2/R_B$. Since the most probable breakup is one in which the neutron and the proton each take half of the available energy, the peak in the energy distribution of the neutrons is at neutron energy $\hat{E}_n$, given by

$$\hat{E}_n = \tfrac{1}{2}(E_d - Ze^2/R_B - 2.2 \text{ MeV}). \quad (1a)$$

Since protons are accelerated outward by the Coulomb field, the corresponding energy for protons, $\hat{E}_p$, is[2]

$$\hat{E}_p = \tfrac{1}{2}(E_d - Ze^2/R_B - 2.2 \text{ MeV}) + Ze^2/R$$
$$= \tfrac{1}{2}(E_d + Ze^2/R_B - 2.2 \text{ MeV}). \quad (1b)$$

By measuring the position of the peak in the energy distribution of the protons, one therefore determines R_B. From the experimental measurements,[3] R_B has been found to be well outside of what is usually considered to be the nuclear radius. When the bombarding energy E is low and the target is of high atomic number Z, R_B is especially large, and it is assumed that the breakup is due to the Coulomb field. As E increases and Z decreases, R_B gets smaller until eventually the breakup must be caused principally by nuclear forces. It was found that the angular correlation between the neutron and proton changes as Z or E is changed: In the region where R_B is large, the neutron and proton come off on the same side of the incident beam (with the proton angle generally larger than the neutron angle), whereas in the region where R_B is small, the neutron and proton tend to be emitted on opposite sides of the incident beam. The change-over occurs for $R_B \simeq 2.5A^{1/3}$ F.

If the values of R_B obtained[3] from (1b) are to be taken seriously, deuteron breakup occurs at radii well outside of the usual nuclear radius. This process therefore promises to yield information on the nuclear potential—as represented, for example, by an optical model potential—at large radii. In order to make such studies quantitative, an accurate theoretical treatment of the problem is necessary. The basic theory has been worked out,[5] but as yet no numerical results are available. However, experimental studies have continued in the hope that theoretical results will be

* Work supported by the National Science Foundation.

[1] F. Udo, Rev. Mod. Phys. **37**, 365 (1965); R. B. Roberts and P. H. Abelson, Phys. Rev. **72**, 1003 (1947); B. L. Cohen and C. E. Falk, *ibid.* **84**, 173 (1951); F. A. Aschenbrenner, *ibid.* **48**, 657 (1955); B. L. Cohen *et al.*, *ibid.* **118**, 499 (1959).

[2] E. W. Hamburger, B. L. Cohen, and R. E. Price, Phys. Rev. **121**, 1143 (1961).

[3] E. C. May, B. L. Cohen, and T. M. O'Keefe, Phys. Rev. **164**, 1253 (1967).

[4] J. R. Oppenheimer, Phys. Rev. **47**, 845 (1935); H. B. Kitchum, Ph.D. thesis, University of Pittsburgh, 1960 (unpublished); S. Dancoff, Phys. Rev. **72**, 1017 (1947).

[5] L. D. Landau and E. Lifschitz, Zh. Experim. i Theor. Phys. **18**, 750 (1948).

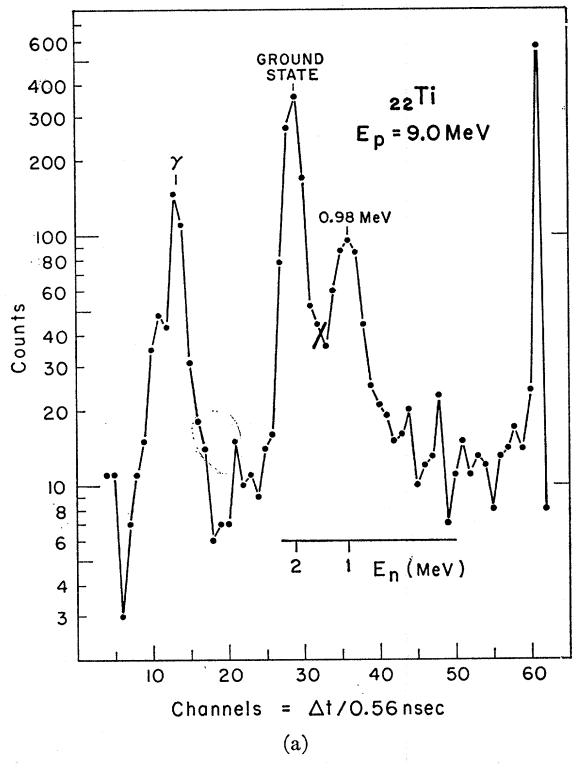

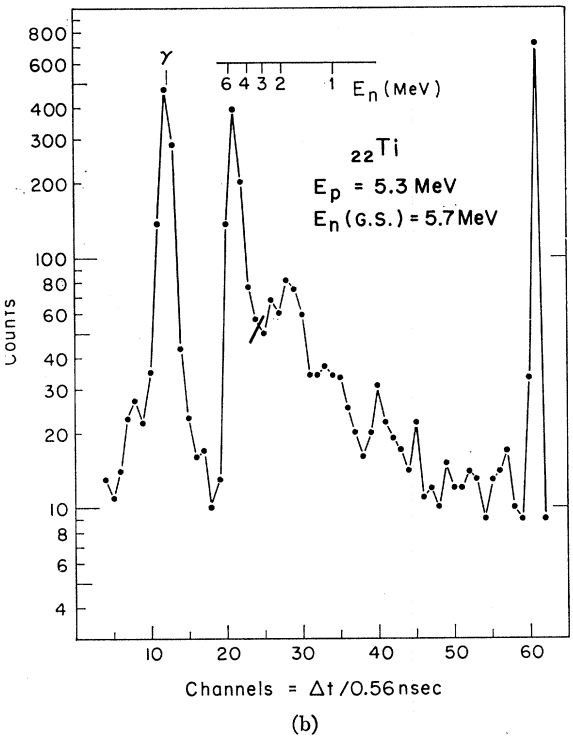

FIG. 1. Cuts across a typical two-dimensional data display. These are plots of total counts versus Δt for two different values of E_p. The energy scale as obtained from the time of flight relative to that of γ rays is shown. Excitation energy of state excited = 11 MeV$-E_p-E_n$.

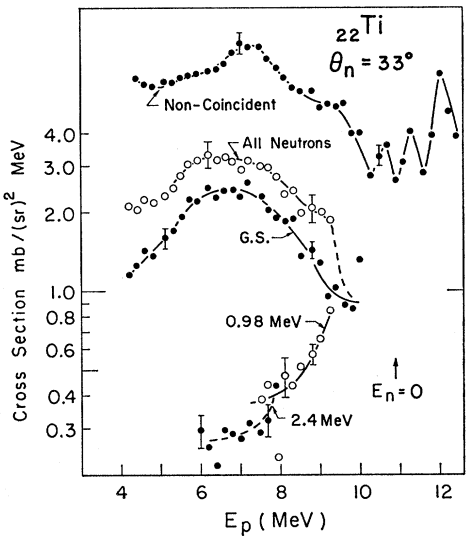

FIG. 2. Differential cross section for emission of a coincident neutron and proton in the bombardment of Ti by 13.6-MeV deuterons. Curves labelled G.S. (ground state) and by energies in MeV are cross sections for exciting those states in the final nucleus, and the curve labelled all neutrons is the total cross section for exciting all states of the final nucleus. The curve labelled "noncoincident" is the energy spectrum of all charged particles (presumably mostly protons) emitted at $-40°$. Arrow labelled $E_n=0$ indicates the sum of E_n+E_p for transitions to the ground state. Angle of proton detector is $-40°$. E_p scale is not corrected for energy loss in the target. Target thickness is 5.9 mg/cm². These data represent an average of two runs.

forthcoming. In one study of this type, Nemets, Pugach, Sokolov, and Strughts[6] found changes in the breakup cross section occurring nonmonotonically with Z and A. In particular, they report that cross sections are larger near the Ca and Ni closed shells, and they interpret this to be due to changes in the diffuseness of the nuclear surface for closed-shell nuclei. We will refer to this as the "Nemets effect."

The work in Ref. 6 is confined to the Ca-Ni region; all data were taken with 13.6-MeV incident deuterons, and they do not include energy measurements on the emitted neutrons and protons. The purpose of this work is, first, to investigate further the Nemets effect by making more detailed measurements in the Ca-Ni region and by extending the study to other mass and energy regions; and second, to use these results to elucidate further some aspects of the deuteron breakup process.

EXPERIMENTAL

The experimental technique has been described in detail previously.[7] Protons are detected by a surface

[6] O. F. Nemets, V. M. Pugach, M. V. Sokolov, and B. G. Struzhko, in Proceedings of the International Symposium on Nuclear Structure, Dubna, USSR, 1968 (unpublished).

[7] B. L. Cohen, E. C. May, and T. M. O'Keefe, Phys. Rev. (to be published).

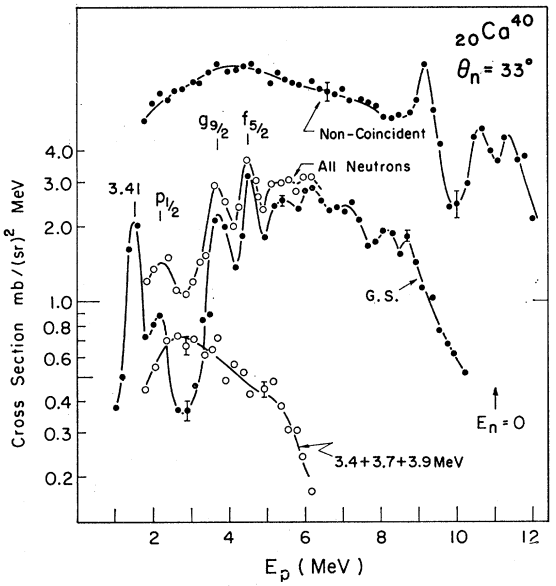

FIG. 3. Differential cross section for emission of a coincident neutron and proton in the bombardment of Ca with 13.6-MeV deuterons. See caption for Fig. 2. Labelling of peaks are l, j assignments from Ref. 9; peak labelled 3.41 is due to excitation of the 3.41-MeV state in Sc^{41} by the (d, n) reaction. Target thickness is 2.7 mg/cm².

barrier detector "sandwich," and their energies are measured by pulse height analysis. Neutrons are detected by a $3\frac{1}{2}$-in.-diam$\times\frac{3}{4}$-in.-thick plastic scintillator, and their energies are determined by time of flight from the difference Δt in the times of arrival of the neutrons and protons at their respective detectors. Flight paths vary from 18 to 50 cm, and the time resolution is about 1 nsec. Data are displayed in a two-dimensional array—proton energy (E_p) versus Δt—so events of interest appear along a curve determined kinematically by the relation

$$E_p+E_n=E(\text{incident})-2.2\ \text{MeV}, \qquad (2)$$

where E_p and E_n are the energies of the proton and the neutron, respectively. Events in which the target nucleus is not left in its ground state are separated as they lie on different curves for which the right side of (2) is reduced.[7]

Two cuts across the two-dimensional array from a typical run are shown in Fig. 1; these are plots of number of counts versus Δt for two different proton energies. In Fig. 1(a) the neutron energy is sufficiently low that the ground state transition is clearly separated from the others. In Fig. 1(b) the high neutron energy, combined with the limited time resolution and flight path, does not allow this separation to be made, but the shape of the plot suggests that the great majority of non-ground-state transitions are to highly excited states which are easily separated. This is confirmed in Fig. 2, which shows the areas under peaks like those in Fig. 1 plotted versus E_p. It is readily seen there that transitions to the low-energy states fall off with decreasing E_p and become negligible at energies where they cannot be resolved from ground-state transitions.

A considerable effort was made to determine absolute cross sections in these experiments. As in the previous work,[3,7] the product of the incident-beam current and the target thickness is measured during data accumulation runs by monitoring deuterons elastically scattered through 30° with a surface barrier detector. In the present work this monitor detector is frequently "calibrated" against incident-beam current in separate runs in which a Faraday cup with a negatively biased guard ring is inserted a short distance beyond the target. In addition, the energy is changed to 14.5 and 11.8 MeV, where the ratio of monitor counts to beam collected in the Faraday cup is measured; since elastic-scattering cross sections at 14.5 and 11.8 MeV have been accurately determined,[8] this gives a check on target thickness and on the over-all method. As a result of these precautions and frequently repeated measurements, it is believed that the relative cross sections reported for different target nuclei are accurate to within about 10%.

RESULTS AND DISCUSSION: Ca-Ni REGION

In order to investigate further the results of Nemets *et al.*, measurements were made for several targets in the Ca-Ni region with 13.6-MeV deuterons, observing the protons at −40° and the neutrons at 27°,

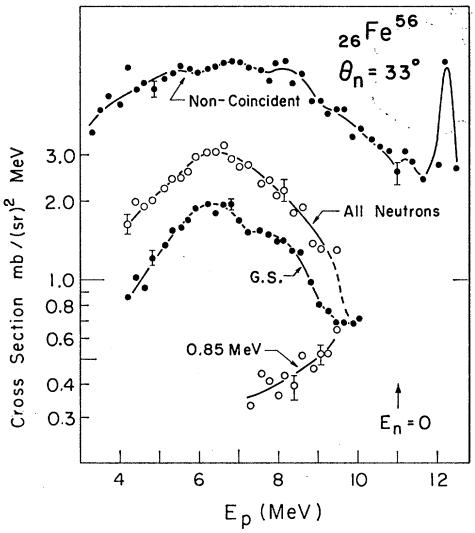

FIG. 4. Differential cross section for emission of a coincident neutron and proton in the bombardment of Fe with 13.6-MeV deuterons. See caption for Fig. 2. Target thickness is 3.4 mg/cm².

[8] G. Mairle and U. Schmidt-Rohr, Max-Planck-Institut für Kernphysik, Heidelberg, Report No. 1651V113 (unpublished); R. K. Jolly, E. K. Lin, and B. L. Cohen, Phys. Rev. **130**, 239 (1963).

33°, and 40°; these are the conditions where the interesting results were obtained in Ref. 6. Proton energy spectra in coincidence with neutrons emitted at 33° are shown in Figs. 2–7 for various target nuclei. In addition to giving results for transitions to the ground and low-energy excited states, they also show the cross sections for protons coincident with all neutrons as obtained by summing over curves like those in Fig. 1, and for all protons without the coincidence requirement. The latter were obtained from accidental coincidences which, because of a special feature of the time-to-pulse height converter, are proportional to the height of the large peak in channel 61 of Fig. 1.

Perhaps the most surprising aspect of these figures is the appearance of sharp structure. In all cases where the curves through the data show peaks, peaking was

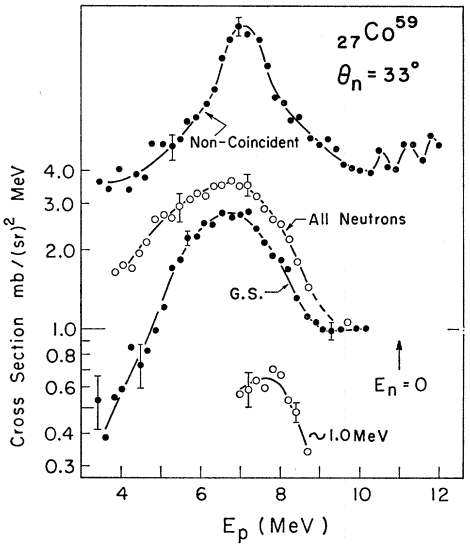

FIG. 5. Differential cross section for emission of a coincident neutron and proton in the bombardment of Co with 13.6-MeV deuterons. See caption for Fig. 2. Target thickness is 7.7 mg/cm^2.

observed in at least two independent runs. The most straightforward explanation of these peaks is that they are due to (d, p) reactions followed by neutron emission, or, analogously, to (d, n) reactions followed by proton emission. In the first case, a (d, p) reaction is essentially a mechanism for inserting a neutron so that it selectively excites states which have large amplitudes of the configuration "target and neutron"; this configuration selectively decays by neutron emission to the target nucleus in its ground state.

The most interesting situation of this type is the $Ca^{40}(d, n)Sc^{41}$ reaction, since the proton separation energy for Sc^{41} is only 1.6 MeV. This means that the E_p region between 1.5 and 5 MeV corresponds to excitation energies in Sc^{41} between 3.1 and 6.6 MeV, which is low enough for individual states to contribute importantly. In fact, the four peaks with lowest E_p in Fig. 3 correspond to excitation by the (d, n) re-

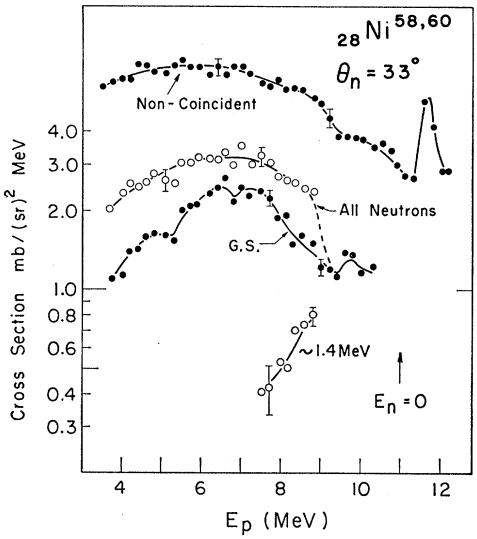

FIG. 6. Differential cross section for emission of a coincident neutron and proton in the bombardment of Ni with 13.6-MeV deuterons. See caption for Fig. 2. Target thickness is 4.5 mg/cm^2.

action of known levels with large proton widths for transitions to the ground state.[9,10] In studies of these states by resonance elastic proton scattering,[9] l, j values as well as Γp were obtained, and the former are shown in Fig. 3.

In all other cases for both (d, n) reactions followed by proton emission and (d, p) reactions followed by neutron emission, the excitation energies of the states

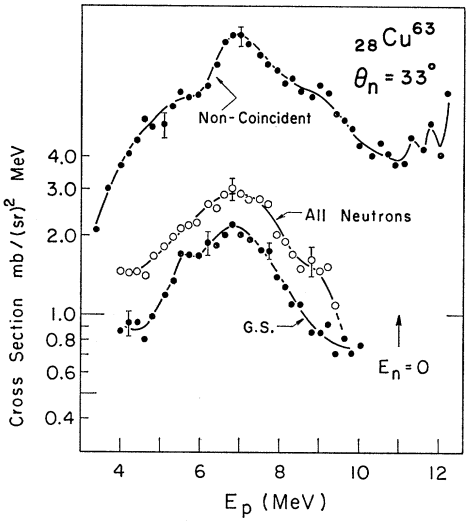

FIG. 7. Differential cross section for emission of a coincident neutron and proton in the bombardment of Cu^{63} with 13.6-MeV deuterons. See caption for Fig. 2. Target thickness is 3.4 mg/cm^2.

[9] C. M. Class, R. H. Davis, and J. H. Johnson, Phys. Rev. Letters **3**, 41 (1959).

[10] G. F. Knoll, J. S. King, and W. C. Parkinson, Phys. Rev. **131**, 331 (1963); H. S. Plendl and F. E. Steigert, *ibid.* **116**, 1534 (1959).

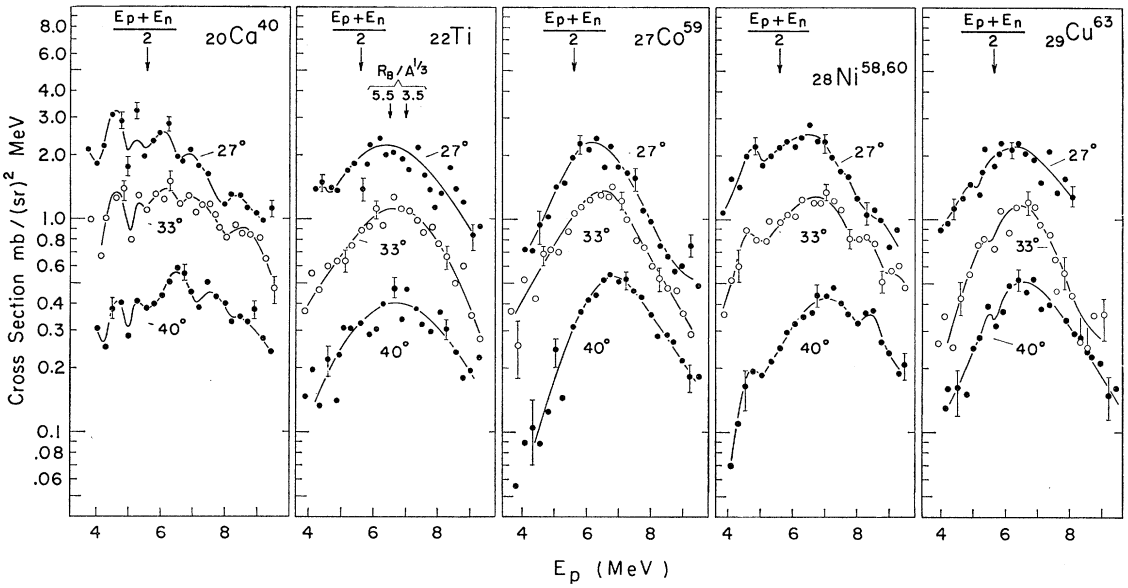

FIG. 8. Differential cross sections for emission of a coincident neutron and proton leaving the final nucleus in its ground state when various targets are bombarded with 13.6-MeV deuterons. θp is $-40°$, and θn is designated for each curve; all data are normalized to the same scale, except the 33° data are $\times\frac{1}{2}$ and the 40° data are $\times\frac{1}{4}$. Scale of $R_B/A^{1/3}$ is calculated from Eq. (1b). These data represent an average of two or more independent runs.

excited by the stripping reactions are so high that we can expect only giant resonance-type groupings of states, whence the peaking is much less striking. However, it is almost certainly present. For example, the peak near 5 MeV for Ni in Fig. 6 was clear on six independent runs, including some on different days and at different angles, and it never failed to appear.

The peaking as we interpret it indicates that all of the data here and hence also in Ref. 6 include important contributions from (d, pn) and (d, np) reactions and are not predominantly from deuteron breakup. Further evidence for this conclusion comes from the noncoincident data of Figs. 2–7. Above the threshold for (d, pn), this is due to ordinary (d, p) reactions, and there is no reason for the number of protons from these reactions to decrease in the first few MeV below the threshold. Moreover, one expects about an equal number of (d, n) reactions, and when the energy of emitted neutrons is low enough, these become (d, np) reactions giving an additional source of protons. Combining these effects, one expects the contribution of protons from stripping reactions in the region around $E_p=8$ MeV to be roughly double that in the region above 11 MeV. We see from Figs. 2–7 that this reasoning would indicate that almost all of the protons are from stripping reactions rather than from deuteron breakup. However, it should be noted that the "noncoincident" curves of Figs. 2–7 include reactions in which neutrons are emitted at all angles, not just at the relatively forward angles studied here. Moreover, since no particle discrimination was used, they may contain important contributions from alpha particles. Therefore one should be wary of accepting the extreme interpretation suggested by the above reasoning, but there can be little doubt that stripping reactions do make an important contribution. And the fact that Ca^{40} and Ni^{58}, the two nuclei for which the large cross sections were the basis of the conclusions in Ref. 6, have more peaks than the others must make us hesitant at this point to accept the Nemets effect.

More direct comparison with Ref. 6 can be made with Fig. 8, which shows measurements with better angular resolution (but poorer statistics) at 27°, 33°, and 40° for all of the nuclei studied. Curves at successive angles are displaced by a factor of two, so the fact that the 33° curves are less than a factor of two below the 27° curves, and more than a factor of two above the 40° curves, means that the angular distributions have a maximum near 33°, in agreement with Ref. 6.

The conclusions of Ref. 6 were based upon the observations that the integrals of (i.e., areas under) these curves, which were all they were able to measure, are larger for Ca^{40} and Ni^{58} by factors of 2.0 and 1.5 than for Co^{59} and Ni^{64}, respectively. While a Ni^{64} target was not available, it would seem that Cu^{63} is equally far from a closed shell and should be equivalent. From Fig. 8 we see that the large areas under the curve for Ca^{40} and Ni^{58} seem to be due more to the widths of the curves than to their heights (i.e., maximum cross sections) and that these extra widths seem to be due largely to the peaks in the energy distributions which we have interpreted as due to stripping reactions. There is no difference outside of experimental error in the maximum cross sections,

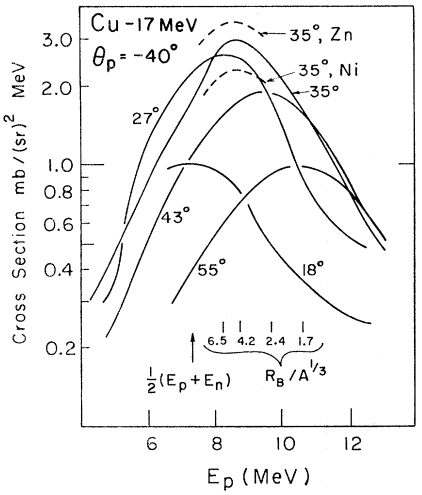

FIG. 9. Differential cross sections for emission of a coincident neutron and proton leaving the final nucleus in its ground state when a Cu target is bombarded by 17-MeV deuterons. Proton detector is at −40° and neutron detector is at angles shown. Data for Zn and Ni are similar except for over-all scale shifts designated by the difference between the three segments of the 35° curve. Scale of $R_B/A^{1/3}$ is calculated from Eq. (1b). These data were not remeasured, so they should be considered approximate.

and any possible differences are certainly much less than factors of 1.5 or 2. From this it would seem that there is little evidence for the Nemets effect in this mass and energy region.

The results of a brief effort to study these nuclei with 17-MeV bombarding energy are shown in Fig. 9, where the data are for Cu^{63}. Data for Zn and Ni were similar except for the total cross sections for which typical differences are shown. These cross-section differences were not carefully checked, but

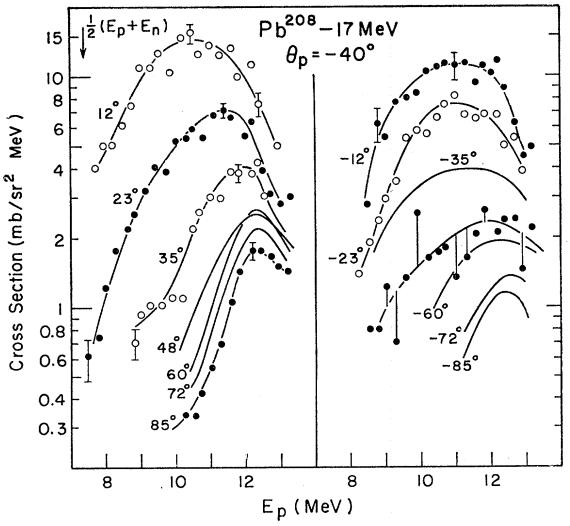

FIG. 10. Differential cross sections for breakup of 17-MeV deuterons by Pb^{208} versus E_p when $\theta p = -40°$ and θn is the angle shown. Data shown are typical. These data were not remeasured, so they should be considered approximate.

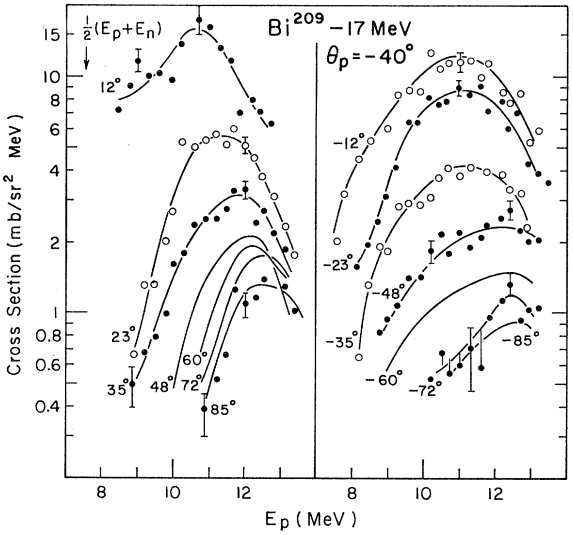

FIG. 11. Differential cross sections for breakup of 17-MeV deuterons by Bi^{209}. See caption for Fig. 10.

the evidence seems to indicate that Ni, if anything, has a *smaller* cross section, which is contrary to the Nemets effect. Since the shape of the energy spectrum changes drastically with angle—a property not expected from stripping reactions—this energy region may be a useful one for studying deuteron breakup. However, it was decided at this point that studies of heavier nuclei would be more clear-cut.

RESULTS AND DISCUSSION: Pb REGION

In heavy nuclei, the large Coulomb barrier strongly reduces the number of protons from (d, pn) and (d, np) reactions in the region of interest for deu-

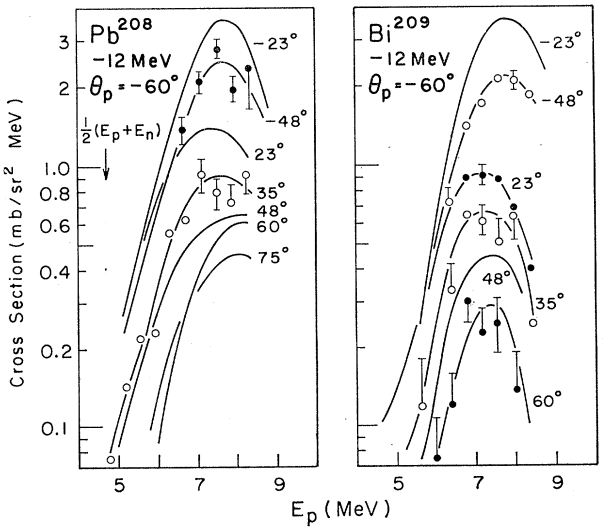

FIG. 12. Differential cross sections for breakup of 12-MeV deuterons by Pb^{208} and Bi^{209} with $\theta p = -60°$. See caption for Fig. 10.

TABLE I. Ratio of deuteron breakup cross sections (σ_{BU}) for Pb^{208} and the other nuclei studied.

E (MeV)	p angle	n angle	$\sigma_{BU}(Bi^{209})/\sigma_{BU}(Pb^{208})$	$\sigma_{BU}(Au^{197})/\sigma_{BU}(Pb^{208})$	$\sigma_{BU}(Pt^{198})/\sigma_{BU}(Pb^{208})$
17	−40°	+48°	0.83±0.05	0.47±0.05	0.47±0.05
17	−40°	+60°	0.75±0.05	0.37±0.05	0.39±0.05
14.5	−40°	+48°	0.75±0.05	0.65±0.10	0.76±0.10
14.5	−40°	+60°	0.85±0.05	0.67±0.05	0.65±0.10

teron breakup,[2,11] thus making it possible to study the latter process more clearly. In addition, the closed shell at Pb^{208} is much more definite than the closed shells at Ca^{40} and Ni, whence we would expect the Nemets effect to be stronger. In addition, absolute cross sections can be determined more reliably because the elastically scattered deuterons which are used in monitoring vary more smoothly with angle and with atomic number than in the lighter nuclei. Therefore studies were made in the Pb region using targets of Pb^{208}, Bi^{209}, Au^{197}, and Pt^{198}. The latter two were chosen because they are away from the closed shell and should clarify possible odd-even differences. Some energy and angular distributions for Pb^{208} and Bi^{209} are shown in Figs. 10, 11, and 12. In all cases, angular distributions are peaked near the forward direction and, as found in Ref. 3, the neutrons and protons are more frequently emitted on opposite sides of the beam at 17 MeV and on the same side of the beam at 12 MeV. The closest analogy in the 17-MeV data with the angular region studied in the lighter nuclei and in Ref. 6 is at neutron angles of about 48° to 60°; here the angular distributions are slowly varying if not peaked, and the energy distribution does not change rapidly with angle. It was therefore decided to study the relative cross sections for deuteron breakup in the four target nuclei at these angles. A similar (but briefer) study indicated that this angular range is also suitable at 14.5-MeV bombarding energy, so data were also obtained there. Since there is apparently no similarly suitable region at 12 MeV and the rate of data accumulation was slowed by the low breakup cross sections and the large elastic scattering cross section, that energy was not used for detailed studies.

The principal effort was directed at obtaining accurate determinations of the cross-section ratio for the various targets and the energy of the peak in the angular distribution. Several independent runs extending over a period of several months were made to determine these. The results are shown in Table I and II.

In Table I, we see a clear indication of a Nemets effect. The breakup cross section for Pb^{208} is definitely larger than for Bi^{209}, and twice as large as for Au and Pt. The Au and Pt cross sections are very similar to one another, even though the former is an odd-A nucleus, while the latter is even-even, so odd-even effects probably cannot explain the Pb-Bi difference.

From Table II, we see that R_B in Fermi, as determined from the peaks in the energy distributions with (1b), is about $2.1A^{1/3}$ at 17 MeV and $2.6A^{1/3}$ at 14.5 MeV. This is in agreement with previous results[3] and it seems qualitatively reasonable, since higher-energy deuterons can more easily penetrate close to the nucleus. However, the Nemets effect can arise only in breakup by nuclear forces, since electric forces must surely vary slowly and monotonically from nucleus to nucleus. The presence of a Nemets effect at 14.5 MeV and the data of Table II would therefore seem to indicate that nuclear breakup is important even for R_B as large as $2.6A^{1/3}$ F—more than twice the nuclear radius. At that distance the usual optical-model potential is less than 0.1% of the Coulomb potential, so this conclusion is very difficult to accept. The only alternative is to conclude that (1b) is not valid.

That derivation is obviously deficient in not including the potentials arising from the nuclear force. If these are treated as real potentials, $-V_d$, $-V_p$, and $-V_n$ for deuterons, protons, and neutrons, respectively, and if we can make the assumption

$$V_d = V_n + V_p, \tag{3}$$

TABLE II. Energy of protons at the peak of their energy distribution, and R_B derived from these energies with (1b).

E (MeV)	p angle	n angle	Bi^{209} $\hat{E}_p$ (MeV)	Bi^{209} $R_B/A^{1/3}$ (F)	Pb^{208} $\hat{E}_p$ (MeV)	Pb^{208} $R_B/A^{1/3}$ (F)	Au^{197} $\hat{E}_p$ (MeV)	Au^{197} $R_B/A^{1/3}$ (F)	Pt^{198} $\hat{E}_p$ (MeV)	Pt^{198} $R_B/A^{1/3}$ (F)
17	−40°	+48°	11.8±0.3	2.3	12.2±0.1	2.1	11.9±0.3	2.2	12.3±0.3	2.0
17	−40°	+60°	12.3±0.1	2.1	12.4±0.1	2.0	12.6±0.3	1.9	12.5±0.3	1.9
14.5	−40°	+48°	9.4±0.5	3.1	9.8±0.3	2.8	9.8±0.3	2.7	10.2±0.3	2.4
14.5	−40°	+60°	10.2±0.3	2.5	10.2±0.5	2.5	10.0±0.3	2.6	10.0±0.3	2.6

[11] B. L. Cohen, J. B. Mead, R. E. Price, K. S. Quisenberry, and C. Martz, Phys. Rev. 118, 499 (1960).

we find, for a point deuteron,

$$\hat{E}_p=\tfrac{1}{2}(E_d-V_C+V_n+V_p-2.2\text{ MeV})-V_p+V_C$$
$$=\tfrac{1}{2}(E_d-2.2\text{ MeV}+V_C+V_n-V_p), \quad (4)$$

where V_C is the Coulomb potential. From (4) we see that if $V_n=V_p$, we again obtain (1b). However, it is well known that there are differences between V_n and V_p. In order to study the effect of these, we rearrange (4) as

$$2\hat{E}_p-E_d+2.2\text{ MeV}=V_C+V_n-V_p. \quad (5)$$

We take V_C as the potential due to a uniform charge distribution with radius $R_C=1.25A^{1/3}$ F, which is

$$V_C=(Ze^2/R_C)[\tfrac{3}{2}-\tfrac{1}{2}(r/R_C)^2], \quad r<R_C$$
$$=Ze^2/r, \quad r>R_C. \quad (6)$$

The best established differences between V_n and V_p are those due to the symmetry energy[12]

$$\Delta V_0=\pm 27\text{ MeV}\times(N-Z)/A=\pm 5.7\text{ MeV in Pb}, \quad (7)$$

where the plus and minus signs refer to neutrons and protons, respectively, and to the velocity dependence in the nucleon-nucleon force,[12] changing the proton potential by

$$\Delta V_0=0.4(Z/A^{1/3})\text{ MeV}=5.5\text{ MeV in Pb}. \quad (8)$$

In these, ΔV_0 is the change in the coefficient V_0 of the Woods-Saxon potential

$$V=\frac{-V_0}{1+\exp(r-R)/a}. \quad (9)$$

Use of (7) and (8) in (9) leads to

$$V_n-V_p=\frac{16.9\text{ MeV}}{1+\exp(r-R)/A}. \quad (10)$$

If we use $R=1.25A^{1/3}$ and[12] $a=0.65$ F and insert (6) and (10) into the right-hand side of (5), we obtain the solid curve of Fig. 13. The left side of (5), with E_p obtained from Table II (except for the 12-MeV data, which are from Fig. 12), is shown by the shaded bands, their width representing the experimental uncertainty, in Fig. 13. Solutions of (5) occur where these bands cross the curve. We see that, in addition to the solution obtained from (1b) and listed in Table II, there is also a solution for $R_B/A^{1/3}$ near 1.3 F. This solution seems much more acceptable in view of the observation of the Nemets effect, especially at 14.5 MeV.

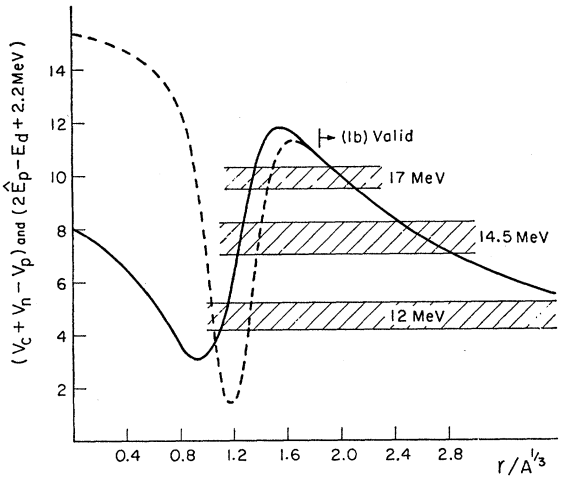

FIG. 13. Determination of R_B. Curve shows right side of Eq. (5) and shaded bands are measurements of the left-hand side of (5) including their uncertainty. Solid curve is calculated with Eq. (10) with $R=1.25A^{1/3}$, $a=0.65$, for both neutrons and protons. Dashed curve is calculated by changing the numerator of Eq. (10) to 8 MeV and using $R=1.25A^{1/3}$ for protons and $R=1.15A^{1/3}$ for neutrons.

There is some reason to believe that the use of (7) and (8) may overestimate the difference between V_n and V_p. If this difference were cut in half, the dip in the curve would be rather slight, so we would no longer have our two solutions. However, a solution near the nuclear surface could then be obtained by making the radius of the proton potential slightly larger than that of the neutron potential. As an example, the dashed curve in Fig. 13 shows V_n-V_p calculated under the assumption that the numerator in (9) is only 8 MeV but $R=1.25A^{1/3}$ for protons and $R=1.15A^{1/3}$ for neutrons. This again gives a solution (indeed two solutions) near the nuclear surface.

CONCLUSIONS AND COMMENTS

The principal conclusions of this work are the following:

(1) There is definitely a Nemets effect in the Pb region, with the closed-shell nucleus having a larger cross section for deuteron breakup than its neighbors.

(2) The existence of this Nemets effect guarantees that nuclear forces, rather than just Coulomb forces, are causing the breakup.

(3) Since Eq. (1b) gives values of R_B too large to be acceptable if the breakup is due to nuclear forces, that equation is not acceptable. A more acceptable procedure is that used in Fig. 13, which indicates that the breakup occurs near what is usually taken to be the nuclear surface.

(4) Studies of deuteron breakup in light nuclei are very suspect because of large contributions from other

[12] F. G. Perey, Phys. Rev. **131**, 745 (1963).

processes. This is especially true in the energy and angular region studied in Ref. 6.

One interesting question about the Nemets effect concerns its sign. One might think that closed-shell nuclei should have a less-diffuse surface than their neighbors and therefore a smaller breakup cross section, contrary to the experimental result. However, Goldhaber[13] has pointed out that a diffuse surface would be a more efficient absorber of nucleons, a process which competes with simple breakup. On the other hand, there is no evidence that cross sections for nucleon absorption processes like (d, p) or (d, n) vary between closed-shell and neighboring nuclei.

[13] M. Goldhaber (private communication).

PHYSICAL REVIEW VOLUME 185, NUMBER 4 20 SEPTEMBER 1969

Giant Resonance in Deformed Nuclei: Photoneutron Cross Sections for Eu^{153}, Gd^{160}, Ho^{165}, and W^{186}†

B. L. BERMAN, M. A. KELLY,* R. L. BRAMBLETT,‡ J. T. CALDWELL, H. S. DAVIS, AND S. C. FULTZ

Lawrence Radiation Laboratory, University of California, Livermore, California 94550

(Received 17 February 1969)

Photoneutron cross sections, including $\sigma[(\gamma, n)+(\gamma, pn)]$, $\sigma[(\gamma, 2n)+(\gamma, p2n)]$, and $\sigma(\gamma, 3n)$, were measured for Eu^{153}, Gd^{160}, Ho^{165}, and W^{186} as a function of photon energy from 8 to 29 MeV. The photon energy resolution varied from less than 300 keV at the lowest to 400 keV at the highest energies, and the data were taken at intervals of 300 keV or less. The source of radiation was the monoenergetic photon beam obtained from the annihilation in flight of fast positrons. The partial cross sections were determined by neutron multiplicity counting, and the average neutron energies for both single- and double-photoneutron events were determined simultaneously with the cross-section data by the ring-ratio technique. Nuclear information extracted from the data includes giant-resonance parameters, integrated cross sections and their moments, nuclear symmetry energies, intrinsic quadrupole moments, and nuclear level density parameters. The data were analyzed to obtain a mean radius parameter $R_0=1.26\pm0.02$ F for these nuclei.

I. INTRODUCTION

THE study of the giant electric dipole resonance in statically deformed nuclei provides both a sensitive test of the classical hydrodynamic model of the nucleus[1,2] and a means of obtaining several important parameters which describe the properties of such nuclei, notably their shape. The hydrodynamic theory, as applied to deformed nuclei,[3–5] makes two major predictions which lend themselves particularly to experimental scrutiny: (1) that the giant resonance is split into two components for spheroidal nuclei, corresponding to dipole vibrations, along the major and minor axes of the spheroid, of two interpenetrating fluids made up of the neutrons and protons in the nucleus; and (2) that the strengths of these two components have the simple ratio of 1:2, corresponding to the number of degrees of freedom for these vibrations. The first condition gives a prescription for the nuclear shape parameters for prolate nuclei, by means of the relation

$$E_m(2)/E_m(1)=0.911\eta+0.089, \quad (1)$$

where $E_m(1)$ and $E_m(2)$ are the lower and higher resonance energies of the two components of the giant resonance and η is the nuclear deformation parameter which is the ratio of the major to the minor axis. The intrinsic quadrupole moment Q_0 for the nucleus then can be computed from the expression

$$Q_0=\tfrac{2}{5}ZR^2(\eta^2-1)\eta^{-2/3}=\tfrac{2}{5}ZR^2\epsilon, \quad (2)$$

where the nuclear radius $R=R_0A^{1/3}$, Z and A are the atomic number and atomic weight, respectively, and the parameter ϵ is the nuclear eccentricity (see Sec. IV). It should be pointed out that while the Coulomb-excitation method for obtaining the quadrupole moment depends upon the transition probability $B(E2)$ according to the formula

$$Q_0^2=(16\pi/5)B(E2) \quad (3)$$

(for even-even nuclei) and hence gives only the magnitude of Q_0, the photonuclear method gives its

† Work performed under the auspices of the U.S. Atomic Energy Commission; a preliminary account of this work appears in Bull. Am. Phys. Soc. **14**, 103 (1969).

* Now at Hewlett-Packard Corp., Palo Alto, Calif.

‡ Now at Gulf General Atomic Inc., San Diego, Calif.

[1] M. Goldhaber and E. Teller, Phys. Rev. **74**, 1046 (1948).

[2] H. Steinwedel and J. H. D. Jensen, Z. Naturforsch. **5a**, 413 (1950).

[3] K. Okamoto, Progr. Theoret. Phys. **15**, 75L (1956).

[4] M. Danos, Nucl. Phys. **5**, 23 (1958).

[5] K. Okamoto, Phys. Rev. **110**, 143 (1958).